Talanta 99 (2012) 909–917

Contents lists available at SciVerse ScienceDirect

Talanta

journal homepage: www.elsevier.com/locate/talanta

Characterization of CMPO and its radiolysis products by direct infusion ESI-MS

G.S. Groenewold [a,*], G. Elias [a], B.J. Mincher [a], S.P. Mezyk [b], J.A. LaVerne [c]

[a] Idaho National Laboratory, 2351 North Boulevard, Idaho Falls, ID 83415-2208, USA
[b] California State University at Long Beach, Long Beach, CA 90840, USA
[c] Radiation Laboratory, University of Notre Dame, Notre Dame IN 46556, USA

ARTICLE INFO

Article history:
Received 16 May 2012
Received in revised form
20 July 2012
Accepted 20 July 2012
Available online 26 July 2012

Keywords:
Direct infusion electrospray
Electrospray ionization mass spectrometry
Metal separations ligand
Radiolytic degradation
Carbamoylmethylphosphine oxide
CMPO
Collision induced dissociation

ABSTRACT

Direct infusion electrospray ionization mass spectrometry (ESI-MS) approaches were developed for rapid identification of impurity compounds formed from octylphenyl-(N,N-(diisobutyl)carbamoyl-methyl) phosphine oxide (CMPO) during alpha and gamma irradiation experiments of this compound in dodecane. CMPO is an aggressive Lewis base, and produces extremely abundant metal complex ions in the ESI-MS analysis that make identification of low abundance compounds that are less nucleophilic challenging. Radiolysis products were identified using several approaches including restricting ion trapping so as to exclude the abundant natiated CMPO ions, extraction of acidic products using aqueous NaOH, and extraction of basic products using HNO_3. These approaches generated protonated, natiated and deprotonated species derived from CMPO degradation products formed via radiolytic cleavages of several different bonds. Cleavages of the amide and methylene–phosphoryl bonds appear to be favored by both alpha and gamma irradiation, while alpha irradiation also appears to induce cleavage of the methylene–carbonyl bond. The degradation products observed are formed from recombination of the initially formed radicals with hydrogen, methyl, isopropyl and hydroxyl radicals that are derived either from CMPO, contacted aqueous nitric acid, or the dodecane solvent.

1. Introduction

Extractant ligands are hydrophobic organic compounds that function as aggressive Lewis bases, forming strong coordination complexes with metal cations. These properties make them useful for the selective separation of radionuclide metals from used nuclear fuel solutions using solvent extraction. One such example is octylphenyl-(N,N-diisobutylcarbamoyl)methyl phosphine oxide (CMPO, Fig. 1), which has been extensively studied as a mixture with tri-*n*-butyl phosphate for the separation of actinides and lanthanides from dissolved nuclear fuel in the TRUEX process (TRansUranic elements EXtraction) [1–8].

In solvent extraction processes it is critical that the partitioning behavior of the solvent system remain constant, otherwise metal separation efficiency and selectivity can be compromised. A potential problem is that the radiation field associated with the radionuclides present in solutions of used nuclear fuel may cause homolytic cleavage of bonds in ligands forming free radicals. Subsequent radical recombination reactions can form radiolytic degradation products that may not have the same selectivity for the formation of coordination complexes [9]. For example, alpha radiation from ^{239}Pu and ^{241}Am caused significant radiation damage to the TRUEX solvent [10], which can result in poorer partitioning of the metal into the organic phase (a lower distribution ratio). Other reports showed improved distribution ratios for TRUEX solvent that had been cleaned up using sodium carbonate, which suggested the formation of acidic compounds during irradiation [11,12]. These examples underscore the importance of understanding the degradation behavior of CMPO in radiation fields under highly acid conditions, in order to exert satisfactory process control. Accordingly the stability of CMPO is thus a key issue, and has been the subject of several research efforts [9].

Chiarizia and Horwitz observed formation of both octylphenylphosphinic acid and methyloctylphenylphosphine oxide in gamma radiolysis experiments in the presence of HNO_3 [13]. They proposed a degradation pathway that involved initial attack on the amide group by hydrolysis, resulting in the formation of octylphenylphosphinylacetic acid and diisobutylamine (Fig. 1d). The acetic acid derivative is unstable and de-carboxylates to methyloctylphenylphosphine oxide. This pathway was consistent with known behavior of amides and phosphine oxides; however they could not rule out homolytic cleavage of CMPO bonds followed by recombination reactions involving cleavage pathways 'b' and 'c'. In a subsequent GC study of degraded CMPO solutions

* Corresponding author. Tel.: +1 208 526 2803; fax: +1 208 526 8541.
E-mail address: gary.groenewold@inl.gov (G.S. Groenewold).

0039-9140/$ - see front matter © 2012 Elsevier B.V. All rights reserved.
http://dx.doi.org/10.1016/j.talanta.2012.07.056

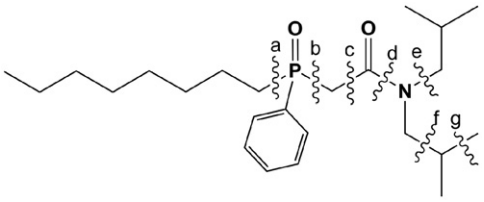

Fig. 1. Degradation pathways previously observed in CMPO radiolysis experiments.

[14,15], radiolytic degradation products were generated by cleavages of the N-isobutyl group ('e'), the amide bond ('d'), C(=O)–CH_2 ('c'), and the CH_2–P(=O) bond ('b'). Dangling bonds formed by the radiolytic cleavage reactions were satisfied by recombination with either H, OH or methyl radicals, and thus significant products were octylphenyl-N-isobutylcarbamoylmethylphosphine oxide, methyloctylphenylphosphine oxide, octylphenylphosphinic acid, and octylphenylphosphinyl acetic acid. Hydrolysis fostered by contact with HNO_3 tended to produce the two acidic products, and there is some uncertainty in the interpretation of the formation of methyloctylphenylphosphine oxide, because it has been reported that this compound can form as a result of thermolysis in the injector of the GC [16].

Mathur and coworkers examined the effects of gamma irradiation and HNO_3 contact on CMPO stability [17], and identified four distinct degradation products, namely methyloctylphenylphosphine oxide, octylphenylphosphinic acid, methylene-N,N-diisobutylcarbamoylmethylphenylphosphinic acid, and (N,N-diisobutylcarbamoyl)-nitromethylphenylphosphine oxide. The first two products were previously observed by Chiarizia and Horwitz in their study of gamma irradiation products [11], and can arise by cleavage pathways 'b' or 'c', followed by combination with either $^{\bullet}H$, $^{\bullet}CH_3$, or $^{\bullet}OH$ radicals. The methylene compound has not been seen elsewhere, but could conceivably be formed by elimination of a heptyl radical followed by recombination with a hydrogen radical at the phosphoryl oxygen atom. The nitro compound could be readily formed by cleavage of a hydrogen radical from the central methylene moiety followed by recombination with a $^{\bullet}NO_2$ radical.

The majority of prior characterization efforts have employed gas chromatography [12,15–17]. Gas chromatography is excellent for analysis of volatile species; however it is not so good for highly functionalized degradation products that have low or negligible vapor pressures, because it requires thermal volatilization in the injector that breaks down analytes. More recently, electrospray ionization mass spectrometry (ESI-MS) has been used [18] because it does not require thermal volatilization or desorption of compounds of interest, and hence it is good for compounds with low P_{vap} values or those that are strongly surface adsorptive as a result of reactive functional groups. Thus, ESI-MS is largely non-intrusive in that it normally does not alter the nature of the solute molecules. We have shown that analyte modification can occur in the case of dithiophosphinic acids, which will oxidatively couple to form disulfides [19]. However we have not observed solute modification for amide- or phosphoryl-containing molecules; a significant example is desferrioxamine, which contains multiple amide and hydroxamate functional groups, and is not modified by ESI-MS analysis [20]. The non-intrusive nature of ESI-MS has also been shown in multiple studies of metal coordination complexes with organophosphoryl ligands, for example ESI-MS characterization of dialkylphosphoric acid–lanthanide complexes [21]. More relevant is the work of Crowe et al. who measured *m/z* values of intact lanthanide coordination complexes of di-*t*-butylphenyl-N,N-diisobutyl CMPO, and that of Stockman in the study of Sr^{2+} complexes with the octylphenyl derivative [22]. Herschbach used ESI-MS to examine lanthanide–CMPO coordination complexes, and showed that accurate stability constants could be extracted from the mass spectrometric data [23]. And ESI-MS has also been used to study CMPO–calixarene–lanthanide complexes, as shown by Lamouroux et al. [24]. However there are no characterization panaceas. One difficulty with ESI-MS is that it tends to produce mass spectra that are dominated by very high abundance ions containing the intact ligands, which can preclude observation of degradation products on account of limitations in dynamic range of the mass analyzers. However, for rapid qualitative identification of degradation products, ESI-MS will have advantages provided the dynamic range issues can be overcome.

In the present study we have examined the bifunctional extractant octylphenyl-N,N-(di-isobutyl)carbamoylmethylphosphine oxide (CMPO). The purpose of the study is to evaluate direct infusion ESI-MS approaches for characterizing ligand impurities, to provide tools that could be especially valuable in radiological environments where minimal sample consumption and manipulation is desirable. These analytical approaches may enable rigorous identification of degradation products arising from alpha and gamma irradiation, which will be critical for identifying mechanistic differences between the two modes of irradiation.

2. Experimental

2.1. Sample origin and irradiation treatment

CMPO was obtained from Strem Chemicals Inc., Newburyport, MA. Stock 0.1 M solutions of CMPO in dodecane were irradiated using steady-state ^{60}Co-γ radiation generated by Nordion Gamma Cell 220E (Ottawa, Canada) with a center-line sample chamber with a dose rate of 7.7 kGy h^{-1}, and temperature of 38 °C. Irradiation doses were based on the known dose rate as determined by the standard decay-corrected Fricke dosimetry, and the duration of irradiation. The samples received γ doses of 8.07, 34.6, 52.6 and 71.2 kGy. In addition, CMPO–dodecane solutions in contact with HNO_3 (1 M–6 M) in a 1:1 ratio were also subjected to gamma irradiation in the same fashion. These samples were biphasic, containing an organic layer and a HNO_3 layer.

CMPO–dodecane solutions were alpha-irradiated using a He-ion beam accelerator at Notre Dame Radiation Laboratory (NDRL). Helium ions were produced by a 9 MV FN-Tandem Van de Graaff generator with a 20 KeV plasmatron source. Particle energy was selected by varying the accelerator terminal voltage, with sufficient energy such that after passing through the cell window into the sample their energy was 5 MeV. This was designed to simulate the α-particle energies produced by actinide decay. The dose rate was determined as the product of the integrated beam current and particle energy. Samples were stirred continuously to ensure uniform dose deposition. Samples received α-irradiation dose equivalent to either 20 or 38.2 kGy.

2.2. Electrospray solutions

The 0.1 M CMPO-dodecane solutions required dilution before analysis because they were too concentrated. Dodecane is not compatible with electrospray, and is not completely soluble in ethanol or methanol (MeOH). However these samples were soluble in a solution of 18% octanol (OcOH) in MeOH. A one-to-ten dilution of the original sample produced a solvent system that was EtOH–OcOH–dodecane in the ratio 74:16:10, allowing all subsequent dilutions to be conducted using only MeOH.

Additional samples were generated by extracting the CMPO–dodecane solutions using 1 mM solutions of either aqueous HNO_3 or NaOH. 1 mL of acid or base was added to an equivalent volume

of the CMPO solution and stirred. After extraction, an aliquot of the aqueous layer was removed using a pipette, and then diluted with MeOH for ESI-MS analysis.

In several experiments, CMPO–dodecane samples were spiked with either pinacolyl methylphosphonic acid (PMPA, Sigma Aldrich, St. Louis, MO, USA) or hexylmethylamine (HMA, Sigma Aldrich, St. Louis, MO, USA). Alcoholic solutions of PMPA or HMA were mixed with the CMPO samples to evaluate detectability of phosphoryl acids and amines in the presence of high CMPO concentrations using the direct ESI-MS and the extraction-ESI-MS approaches.

2.3. Electrospray ionization mass spectrometry (ESI-MS)

The instrument utilized in these experiments was a modified Thermo LCQ-DECA XP Max quadrupole ion trap electrospray ionization mass spectrometer. The ESI source was re-positioned from the conventional orthogonal orientation such that the ESI spray was co-axial with the aperture of the sampling cone of the ESI source [25,26]. The distance between the ESI spray capillary and the sampling cone aperture was approximately 3.5 mm.

Typical settings for the ESI source were sheath gas flow = 900 cm^3/min, and ESI flow = 7–8 μL/min. N_2 was used as the sheath gas, and was admitted together with the ESI flow in a coaxial arrangement such that upon exiting the ESI capillary, the ESI flow was jacketed by the sheath gas. The ESI source was fitted with a gas flow meter that enabled measurement.

For positive ion analysis, ESI potential V_{ESI} was 3.5–4.2 kV, adjusted up or down by a few hundred V to stabilize the Taylor cone. Key parameters for the ion trap mass spectrometer included the $V_{\text{transfer capillary}} = 46$ V, and $V_{\text{tube lens offset}} = 35$ V. For negative ion analysis, ESI potential V_{ESI} was 2.75 kV, $V_{\text{transfer capillary}} = -90$ V, and $V_{\text{tube lens offset}} = -100$ V. The transfer capillary temperature was typically operated at 125° C. Experiments were conducted using the automatic gain control, with a target full value of 2.1×10^7 ions.

The mass spectra of these CMPO/dodecane samples tended to be dominated by the $[(CMPO)_2Na]^+$ complex cation at m/z 837, and $[(CMPO)Na]^+$ at m/z 430. Accumulation of these ions made observation of ions at lower m/z values difficult, because the heavier ions are trapped near the center of the ion trap and their space charge tends to decrease the trapping efficiency of low abundance lighter ions. To observe lower abundance ions, the ion trapping was restricted to exclude the very abundant, high mass ions. For example by limiting the upper m/z range to values < 830, $[(CMPO)_2Na]^+$ was not accumulated, which enabled observation of low-abundance adduct ions having m/z values between the mono- and bis-CMPO complexes. By further limiting the upper m/z range to < 400, monomeric CMPO species were not accumulated, which enabled observation of low-abundance ions with lower m/z values $<$ mono-CMPO complexes. Even using this strategy, the observation of ions with $m/z < 200$ was still difficult. To trap these ions, the low mass range trapping option on the LCQ was employed, typically trapping ions from m/z 25 to 200.

3. Results

3.1. Direct infusion electrospray of unirradiated CMPO.

Direct electrospray of CMPO–dodecane solution was problematic because the solvent does not readily carry surface charge and has a slow evaporation rate. A solution compatible with ESI was generated by dissolving the CMPO–dodecane solutions in an 18% 1-octanol–methanol solution. Serial dilutions of the initial standard could then be conducted using methanol alone. The positive ion ESI mass spectrum was dominated by CMPO cationized with Na^+ at m/z 430 and 837 which correspond to $[(CMPO)_{n=1,2}Na]^+$ (Fig. 2, Table 1) [2]. A low abundance tris-complex was also formed at m/z 1244. The formation of cluster ions such as $[(CMPO)_{n=2,3}Na]^+$ may be facilitated by the operating characteristics of the quadrupole ion trap, specifically longer ion residence times (several hundred milliseconds or more) and high pressures. However, similarly abundant cluster ions have been recorded using a time-of-flight mass spectrometer that has a

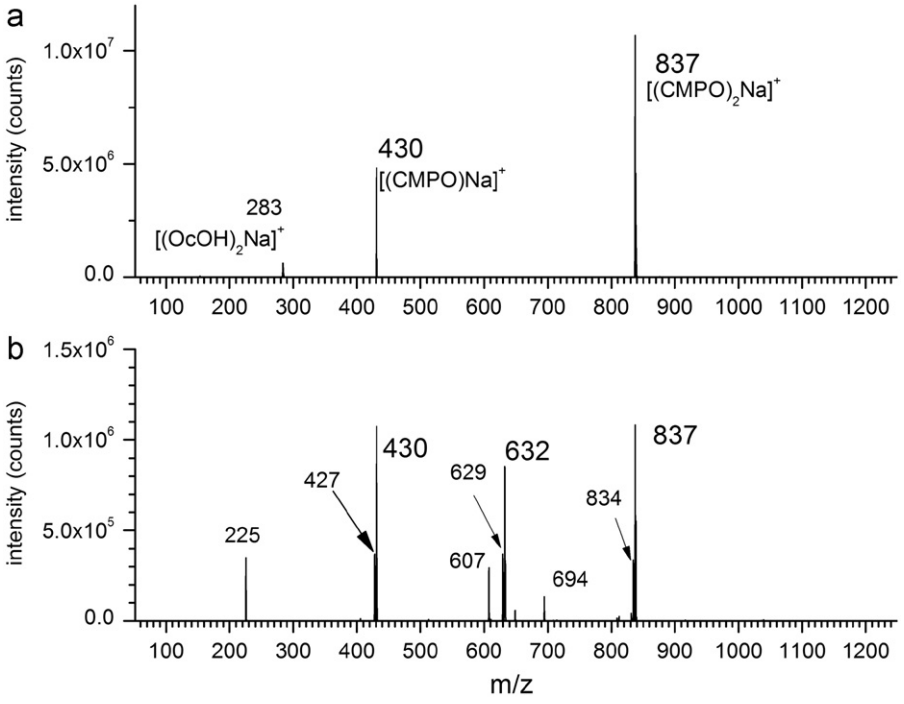

Fig. 2. (a) Positive ESI-MS of un-irradiated CMPO, electrosprayed from an OcOH–EtOH solution. (b) Positive ESI-MS analysis of a solution of CMPO (0.009 mM) and PMPA (0.18 mM). Analysis of the methanolic solution (organic phase, i.e. without extraction).

Table 1
Prominent ions observed in the positive ion ESI mass spectra of the CMPO samples, and their proposed compositions.

m/z	ESI experiment		
	standard CMPO	**CMPO+PMPAH**	**CMPO+HMA**
55	$[(MeOH)Na]^+$	$[(MeOH)Na]^+$	$[(MeOH)Na]^+$
69	$[(EtOH)Na]^+$	$[(EtOH)Na]^+$	$[(EtOH)Na]^+$
87	$[(MeOH)_2Na]^+$	$[(MeOH)_2Na]^+$	$[(MeOH)_2Na]^+$
116			$[(HMA)H]^+$
153	$[(OcOH)Na]^+$	$[(OcOH)Na]^+$	$[(OcOH)Na]^+$
185	$[(MeOH)(OcOH)Na]^+$	$[(MeOH)(OcOH)Na]^+$	$[(MeOH)(OcOH)Na]^+$
199	$[(EtOH)(OcOH)Na]^+$	$[(EtOH)(OcOH)Na]^+$	$[(EtOH)(OcOH)Na]^+$
225		$[(PMPANa)Na]^+$	
278			$[(NaNO_3)_3Na]^+$
283	$[(OcOH)_2Na]^+$	$[(OcOH)_2Na]^+$	$[(OcOH)_2Na]^+$
363			$[(NaNO_3)_4Na]^+$
408	$[(CMPO)H]^+$	$[(CMPO)H]^+$	$[(CMPO)H]^+$
427		$[(PMPANa)_2Na]^+$	
430	$[(CMPO)Na]^+$	$[(CMPO)Na]^+$	$[(CMPO)Na]^+$
448			$[(NaNO_3)_5Na]^+$
523			$[(CMPO)(HMA)Na]^+$
533			$[(NaNO_3)_6Na]^+$
607		$[(PMPANa)_2(PMPAH)Na]^+$	
618			$[(NaNO_3)_7Na]^+$
629		$[(PMPANa)_3Na]^+$	
632		$[(CMPO)(PMPANa)Na]^+$	
703			$[(NaNO_3)_8Na]^+$
788			$[(NaNO_3)_9Na]^+$
815	$[(CMPO)_2H]^+$	$[(CMPO)_2H]^+$	$[(CMPO)_2H]^+$
834		$[(PMPANa)_4Na]^+$	
837	$[(CMPO)_2Na]^+$	$[(CMPO)_2Na]^+$	$[(CMPO)_2Na]^+$
873			$[(NaNO_3)_{10}Na]^+$
900			$[(CMPO)_2(HNO_3)Na]^+$, covalent complex
958			$[(NaNO_3)_{11}Na]^+$
1043			$[(NaNO_3)_{12}Na]^+$
1128			$[(NaNO_3)_{13}Na]^+$
1213			$[(NaNO_3)_{14}Na]^+$
1244	$[(CMPO)_3Na]^+$	$[(CMPO)_3Na]^+$	$[(CMPO)_3Na]^+$

much shorter residence time, which suggests that the cluster ions are characteristic of the ESI process, and are not formed as a consequence of the type of mass analyzer used. The production of mainly metalated species is a feature of the strongly nucleophilic CMPO in the direct infusion ESI-MS experiments. Na^+ was not deliberately present in this experiment; however Na^+ has a well-established reputation as a nearly ubiquitous, adventitious contaminant in ESI-MS experiments, and has proven to be very difficult to eliminate from the analytical process. In instances where adventitious or contaminant metals are more scarce, the protonated complex $[(CMPO)H]^+$ was observed in abundance at *m/z* 408. Several other low abundance ions are observed, notably *m/z* 153 and 283 which correspond to natiated octanol clusters $[(OcOH)_{n=1,2}Na]^+$. There was no evidence for any modification of the CMPO in the analysis of standard solutions, indicating that CMPO is not adversely affected by the alcohol spray solution during the ESI process. Similarly, ESI-MS of pinacolylmethylphosphonic acid and hexylmethylamine showed no modification (vide infra), supporting the assertion that the analysis is not changing the ensemble of organics present in the samples.

Additional benchmark spectra were acquired by limiting ion trapping to *m/z* values <800 thereby excluding $[(CMPO)_2Na]^+$ from the ion trap (Fig. S1) and to <405 to exclude $[(CMPO)Na]^+$ (Fig. S2). This enabled observation of low abundance ions, notably at *m/z* 648, 528, 339 and 311 that are derived from impurities either in the mass spectrometer or the samples. Limiting ion trapping to *m/z* values <200 enables observation of the low mass ions in the spectrum (Fig. S3), which reveals natiated clusters of methanol, ethanol and octanol at *m/z* 55, 69, 87, 153, 185, and 199. Negative ion analysis acquired using the ESI-ion trap displayed very few peaks, the most notable an ion at *m/z* 406 that corresponds to deprotonated CMPO (Fig. S4). This ion is in low abundance, indicating low formation efficiency.

Formation of organophosphinic acids from CMPO has occurred in prior studies [13], and hence it was important to measure small quantities in the presence of a large quantity of CMPO. Pinacolyl methylphosphonic acid (PMPAH) was added as a surrogate organophosphoryl acid to unirradiated CMPO at equimolar concentrations (0.05 mM in both CMPO and PMPAH) and then analyzed. The positive ESI-MS spectrum was again dominated by *m/z* 430 and 837 (Fig. S5), but low abundance ions corresponding to $[(CMPO)_{n=1,2}(PMPANa)Na]^+$ were seen at *m/z* 632 and 1039, and indicated that cluster ions intermediate between the two dominant CMPO peaks can be used to identify impurities. When the relative concentrations were adjusted so that the concentration of PMPAH was a factor of $\sim$20 greater than that of CMPO (0.18 mM versus 0.009 mM), positive ESI-MS analyses contained abundant ions from both components (Fig. 2b). Peaks at *m/z* values of 225, 427, 629 and 831 correspond to the general formula $[(PMPANa)_{n=1-4}Na]^+$ and *m/z* 607 is likely the result of H-for-Na substitution (Table 1). The $[(CMPO)(PMPANa)Na]^+$ at *m/z* 632 is much more intense compared to the equimolar experiment, as is *m/z* 834, which corresponds to $[(CMPO)(PMPANa)_2Na]^+$. The fact that CMPO generates much more intense ions by ESI compared to PMPAH shows that ion intensities cannot be directly related to concentration. Measurement of concentrations would be highly desirable, but would require knowledge of the ESI response of the degradation products relative to CMPO. Alternatively isotopically labeled internal standards of CMPO and its degradation products could be used for more accurate measurement of concentration values, and these approaches represent topics for future study.

The relative intensity of the electrosprayed ions derived from acidic components could be enhanced by extracting the CMPO solutions (0.1 mM in dodecane) with an equal volume of 1 mM NaOH. An aliquot of the aqueous phase was diluted 1:1 with MeOH and then analyzed directly using direct infusion ESI-MS. A very abundant ion at *m/z* 225 that corresponded to $[(PMPANa)Na]^+$ was observed, as were clusters of this ion with additional (PMPANa) molecules which account for *m/z* 427, and 629 (Fig. S6). The low abundance ion at *m/z* 115 is $[(EtOH)_2Na]^+$, which originated from the solvent used for the PMPA. PMPA is transferred to the aqueous base and is readily detected by direct infusion, which suggested similar behavior for other organophosphoryl acids. The natiated CMPO species at *m/z* 430 and 837 showed that some of the CMPO is also partitioning into the NaOH phase.

The anion ESI-MS analysis of the NaOH extract produced the anticipated $[PMPA]^-$ at *m/z* 179, which was confirmed by MS^2 which formed *m/z* 95 by loss of C_6H_{12} as has been previously demonstrated (Fig. S7) [27].

Since basic products are also expected from radiolysis of CMPO, a simple extraction with 1 mM HNO_3 was employed, and initially tested using a 1 mM CMPO–dodecane solution amended with 0.1 mM hexylmethylamine (HMA) as a surrogate. A 1 mL aliquot of this solution was extracted using the same volume of 1 mM HNO_3 for about 90 s, at which point the lower (aqueous HNO_3) layer was removed using a syringe, diluted 1:1 with MeOH, and analyzed by direct infusion. The base peak in the positive ion mass spectrum was $[(CMPO)H]^+$ at *m/z* 408 (Fig. S8), which showed that some of the CMPO partitioned into the HNO_3 layer. The low abundance *m/z* 237 corresponds to $[(C_8H_{17})(C_6H_5)PO]^+$, which is likely generated by fragmentation of *m/z* 408 in this experiment. The sodium that is present is not complexing with CMPO, but instead appears to be scavenged by nitrate: the low abundance ions at *m/z* 278, 363, 448, 533, 618, 703, 788, 873, 958, 1043, 1128 and 1213 are sodium nitrate cluster ions having the general formula $[(NaNO_3)_{n=3-14}Na]^+$. HMA was observed, both as the protonated molecule at *m/z* 116, and

as a complex with CMPO at *m/z* 523, which showed that the pH 3 acid extraction was removing basic components from the dodecane solution.

A significant ion was observed at *m/z* 900, which nominally corresponds to $[(CMPO)_2(HNO_3)Na]^+$; such a composition would normally be interpreted in terms of a non-covalent complex, i.e. a cluster ion similar to many that are formed in electrospray. MS^2 of *m/z* 900 support this idea furnishing an ion at *m/z* 837 resulting from loss of 63 u, which must be HNO_3 (Fig. 3). Subsequent MS^3 of the *m/z* 837 product ion produced *m/z* 708 by loss of 129 u, which corresponds to elimination of diisobutyl amine (DiBA). This ion hydrates in the ion trap, reacting with adventitious H_2O to form *m/z* 726. MS^4 of *m/z* 708 eliminated 129 u (a second DiBA) to form a product ion at *m/z* 579, which also hydrates to form *m/z* 597. Attempts at further fragmentation were not successful.

Since $[(CMPO)_2Na]^+$ is formed at *m/z* 837 in the direct ESI-MS analyses of CMPO, its formation by elimination of HNO_3 from the *m/z* 900 ion suggests this might also be occurring. However the MS^3 fragmentation of *m/z* 837 shows that this is not the case. The serial elimination of two DiBA molecules does indicate that the complex contains CMPO-derived components. However, the fact that the *m/z* 837 fragment does not eliminate intact CMPO to form *m/z* 430 is surprising, since this is how the vast majority of Na^+-bound dimers fragment. The MS^2 of *m/z* 837 formed directly by electrospray produces *m/z* 430 (loss of intact CMPO) and nothing else (Fig. 3d). The elimination of DiBA from the version of *m/z* 837 formed from *m/z* 900 shows that it cannot be a sodium bound cluster, and instead must be a covalently bound CMPO dimer that partitions into HNO_3 and shows up in the ESI analysis as a natiated molecule.

The abundant formation of $[(CMPO)H]^+$ at *m/z* 408 in the ESI mass spectrum of the HNO_3 extract afforded the opportunity to measure its collision induced dissociation reactions, which provide benchmark dissociation behavior for other CMPO-related ions. $[(CMPO)H]^+$ fragments by three competing reactions that produce abundant ions at *m/z* 352, 279 and 237 (Fig. S9). The neutrals eliminated in these reactions are butene, DiBA, and diisobutyl acetamide (DiBAA), respectively (Fig. 4). At the MS^3 stage, the fragment ion at *m/z* 352 eliminates 74 u (perhaps $H_2O+C_4H_8$), while octene is eliminated from *m/z* 237.

Dissociation of natiated CMPO $[(CMPO)Na]^+$ (*m/z* 430) only produces low abundance fragment ions, which is probably the result of greater stability of the coordination complex, and because elimination of Na^+ would produce an ion at *m/z* 23 that is difficult to observe using typical MS^2 parameters in the ion trap. Nevertheless, formation of *m/z* 301 and a lower abundance *m/z* 277 is observed (Fig. S10). The former product arises from elimination of DiBA (Fig. S11), while the *m/z* 277 ion does not have a straightforward explanation but could arise from elimination of octene and a butenyl radical.

3.2. Screening γ-irradiated CMPO

Positive ion analysis of gamma irradiated samples with (34.6, 71.2 kGy) showed very little evidence for radiolytic damage to CMPO, other than a few very low abundance ions that might

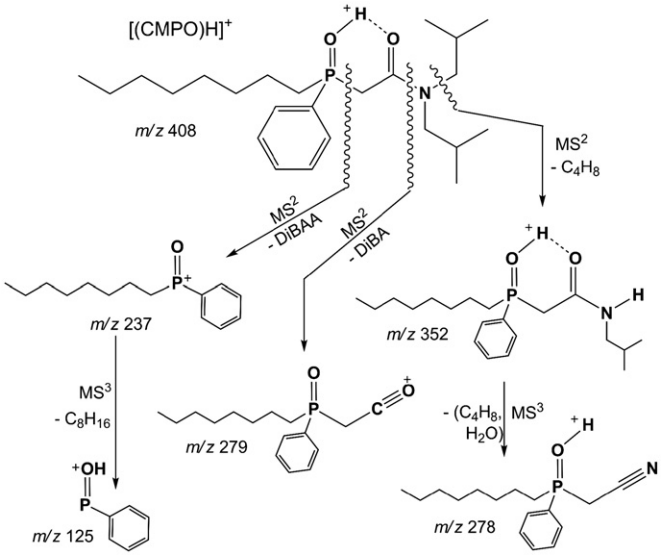

Fig. 4. MS^2, MS^3 dissociation reactions of $[(CMPO)H]^+$ *m/z* 408.

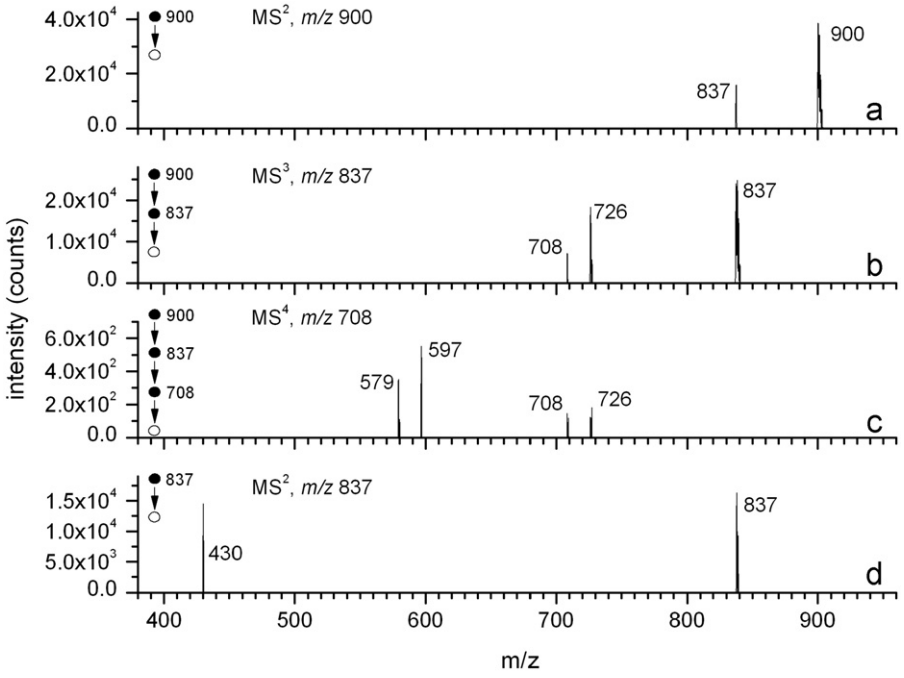

Fig. 3. (a) MS2 of the complex at *m/z* 900, (b) MS3 of *m/z* 837, (c) MS4 of *m/z* 708, and (d) MS2 of *m/z* 837 formed directly by ESI.

indicate formation of CMPO conjugates (Fig. S12). Positive ESI-MS analysis of an alcoholic solution of the organic (dodecane, 10 μM CMPO) phase produced dominant natiated CMPO-containing ions at *m/z* 431, 837 and 1244. Restricting ion trapping to between *m/z* 435 and 830 revealed two peaks *m/z* 507 and 648 (non-radiolytic impurities in the CMPO) and other low abundance ions at *m/z* 708 and 542 (Fig. S13). We suspect that the latter are CMPO conjugates formed from radiation induced radicals that later recombine to form larger molecules, as hypothesized in Fig. S14: *m/z* 708 is 129 u (DiBA) less than the Na-bound dimer at *m/z* 837, suggesting that combination of $[CMPO–(N(iBu)_2)]^{\bullet}$ with $[CMPO–H]^{\bullet}$ might account for this ion. In the same fashion, radical recombination of $[C_8H_{17}]^{\bullet}$ with $[CMPO–H]^{\bullet}$ would produce a molecule that when natiated would account for *m/z* 542. The negative ion analyses contained only very low abundance ions, such as *m/z* 254^- that may be $[(DiBA)(NO_3)_2H]^-$; this assignment is supported by the MS^2 experiment described below.

Analyses of NaOH extracts of gamma-irradiated CMPO showed notable CMPO in the form of $[(CMPO)_{n=1,2}Na]^+$ at *m/z* 430 and 837 (the spectra were nearly identical to those generated by analysis of the organic layer, see Fig. S12). However, a low abundance ion at *m/z* 601 was also seen, which becomes much more prominent when the mass range is restricted to $>$ *m/z* 800. The MS^2 analysis shows that *m/z* 601 is an adduct that dissociates by loss of 171 u to form $[(CMPO)Na]^+$ at *m/z* 430 (Fig. S15); this eliminated fragment corresponds to the molecular mass of DiBAA. The presence of DiBAA was supported by mass spectra acquired with ion trapping restricted to $<$ *m/z* 420: *m/z* 194 and 365 are consistent with $[(DiBAA)Na]^+$ and $[(DiBAA)_2Na]^+$. Negative ion analyses furnished a range of ions (Fig. S16), the most prominent of which is *m/z* 253, deprotonated octylphenylphosphinic acid (OPPAH). MS^2 dissociation furnished *m/z* 175, loss of 78 u that is normally associated with C_6H_6, consistent with the proposed structure shown in Fig. 5.

The ion at *m/z* 346 can be rationalized as the conjugate base of an acidic CMPO derivative in which the phenyl group is replaced by hydroxy (Fig. 6), an idea supported by MS^2 which produced a sole fragment at *m/z* 217, corresponding to elimination of 129 u (DiBA) and consistent with the proposed composition (Fig. S16c). The ion at *m/z* 406 logically corresponds to CMPO deprotonated by the NaOH base (Fig. 7). MS^2 of this ion proceeds by elimination of 129 u (DiBA), and forms *m/z* 277 (Fig. S16d). The ion at *m/z* 422 likely corresponds to a hydroxylated version of CMPO (Fig. 7) which has been observed in prior studies [18].

The analyses of acid extracts of the gamma-irradiated samples generated results similar to those measured for a set of acid-contacted, gamma-irradiated samples, the salient difference being that the latter contained degradation products that were significantly more abundant and thus easier to measure. In this study

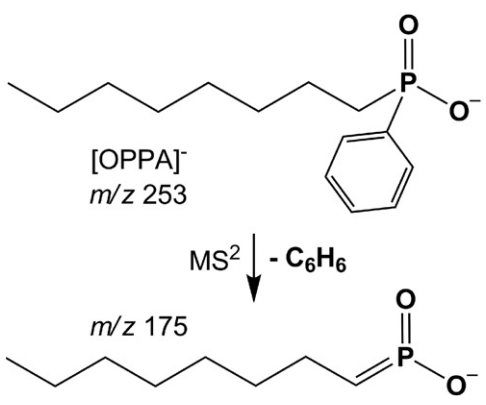

Fig. 5. Proposed fragmentation observed in MS^2 for $[OPPA-H]^-$.

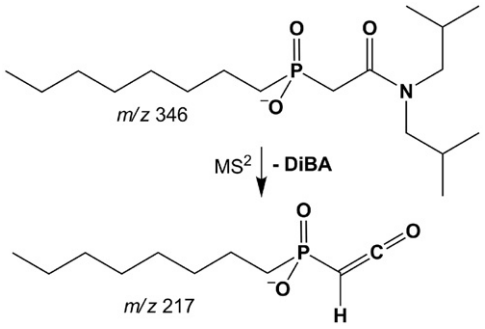

Fig. 6. Structure proposed to account for ion at *m/z* 346, and fragmentation to form *m/z* 217.

CMPO–dodecane solutions were gamma-irradiated while in contact with an equal volume of 3 M HNO_3, and so these samples were biphasic. Direct infusion ESI-MS of the diluted organic layer generated the natiated CMPO clusters $[(CMPO)_{n=1-3}Na]^+$ at *m/z* 430, 837 and 1244 (spectra were nearly identical to Fig. S12). Limiting ion trapping to *m/z* values between 435 and 830 (i.e., excluding the CMPO monomer and dimer species, see Fig. S13) produced a weak spectrum that nevertheless contained adduct ions at the same *m/z* values seen in the analyses of the gamma-irradiated CMPO in Section 3.3, i.e. *m/z* 542 and 708.

In contrast, analyses of the HNO_3 phase were characterized by an abundant $[(CMPO)H]^+$ at *m/z* 408 (Fig. 8a); in this case protonated species are observed rather than natiated, reflecting the very high proton concentration in the solution. The second most abundant peak was *m/z* 537 corresponding to $[(CMPO)(DiBA)H]^+$, an assignment supported by the MS^2 elimination of 129 u (DiBA) to form $[(CMPO)H]^+$ at *m/z* 408 (Fig. 8b). Other higher *m/z* ions are also likely indicative of adducts. The ion at *m/z* 481 most likely corresponds to $[(CMPO)(isobutylamine)H]^+$, and *m/z* 422 a methylated CMPO derived from recombination of the $[CMPO-H]^{\bullet}$ and $[CH_3]^{\bullet}$ radicals.

Low abundance *m/z* 352 and 297 are ascribed to CMPO radiolysis products. *M/z* 352 is protonated octylphenyl(N-isobutyl)carbamoylmethyl phosphine oxide, which is formed by cleavage 'e' (Fig. 1) resulting in loss of an isobutyl group [18]. MS^2 spectra are consistent with this assignment: *m/z* 352 eliminates H_2O to form *m/z* 334, and a dominant fragment ion at *m/z* 278 via serial loss of C_4H_8 (Fig. S17, Fig. 9). The resulting ion then eliminates 41 u in a MS^3 experiment corresponding to loss of C_2H_3N to form $[(C_8H_{17})(C_6H_5)P{=}O]^+$ at *m/z* 237, a highly diagnostic signature for a CMPO-derived molecule. The identity of this ion is consistent with the MS^4 fragmentation which eliminated 112 u corresponding to C_8H_{16}, and furnishing the protonated phenyl phosphoryl ion at *m/z* 125.

The low abundance *m/z* 297 corresponds to octylphenylphosphinyl acetic acid, which would be formed by cleavage of the carbonyl-N bond 'd' (Fig. 1), and recombination with $^{\bullet}OH$. This conclusion is in accord with the MS^2 of the protonated molecule which showed the expected loss of H_2O to form *m/z* 279 (Fig. S18), and MS^3 fragmentation showed further loss of 42 u, in this case corresponding to ketene $H_2C{=}C{=}O$ to form *m/z* 237, which is highly diagnostic for compounds derived from CMPO. These fragmentations are consistent with the dissociation scheme in Fig. 10.

At lower *m/z* values, three amine compounds and their complexes are notable (Fig. S19). *M/z* 130 corresponds to protonated diisobutyl amine, and MS^2 of this ion results in elimination of C_4H_8 to furnish a fragment ion at *m/z* 72 (Fig. S20). The largest ion in this region of the mass spectrum is *m/z* 144, which corresponds to protonated methyldiisobutylamine, a conclusion consistent with the elimination of C_4H_8 in the MS^2 spectrum (Fig. S21). This

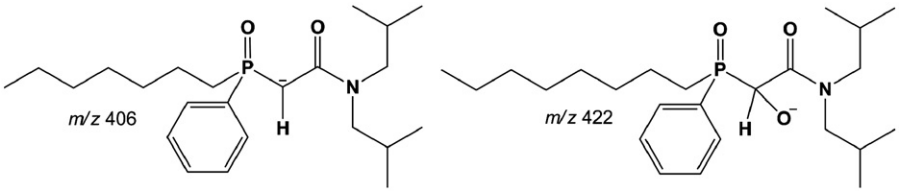

Fig. 7. Ion structures proposed for anions at *m/z* 406 and 422 observed in the direct infusion spectrum of the NaOH extract of gamma-irradiated CMPO.

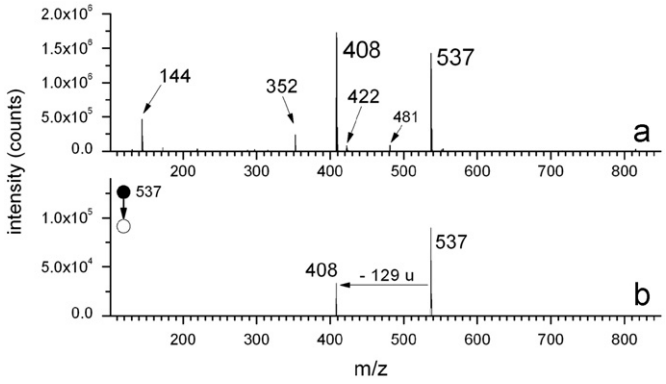

Fig. 8. (a) Direct infusion ESI-MS of the HNO_3 layer, CMPO gamma irradiated in contact with HNO_3. (b) MS2 of *m/z* 537.

compound must be formed from recombination of a diisobutyl amine radical with a methyl radical. The MS^2 and MS^3 spectra of *m/z* 172 identify it as protonated propyldiisobutylamine (Fig. S22): both C_4H_8 and C_3H_6 are competitively eliminated in the MS^2 experiment, generating *m/z* 116 and 130, respectively. MS^3 of *m/z* 116 results in elimination of another C_4H_8 to produce *m/z* 60, which corresponds to protonated propylamine. Recombination of the diisobutyl amine radical and the isopropyl radical provides a likely pathway for formation of this compound. Proton-bound dimers of these species are seen at *m/z* 287 ($[(MDIBA)_2H]^+$) and 315 ($[(MDiBA)(PDiBA)H]^+$). MS^2 of *m/z* 287 eliminates 143 u and generates $[(MDiBA)H]^+$ at *m/z* 144 (Fig. S19b). MS^2 of *m/z* 315 competitively dissociated to form $[(PDiBA)H]^+$ and $[(MDiBA)H]^+$ at *m/z* 172 and 144, respectively (Fig. S19c), favoring $[(PDiBA)H]^+$, a result in accord with its higher proton affinity.

The anion analysis of the HNO_3 layer showed principally ions at *m/z* 125 and 188 that correspond to the series $[(HNO_3)_{n=1,2}H]^+$ (Fig. S23). The ion at *m/z* 254 dissociated by loss of 129 u forming *m/z* 125. This suggests that *m/z* 254 is $[(DiBA+H)(NO_3)_2]^-$, which undergoes elimination of neutral DiBA to form $[(NO_3)_2H]^-$.

3.3. Screening α-irradiated CMPO

CMPO samples in dodecane were also irradiated using a helium ion beam (α particles). MS analyses showed that natiated CMPO and its cluster dimer at *m/z* 430 and 837 were generated along with $[(OcOH)_2Na]^+$ and $[(OcOH)Na]^+$ at *m/z* 283 and 153 (Fig. S24). *M/z* 630 is also observed, and is an adduct with $[(CMPO)Na]^+$ as indicated by elimination of 200 u to furnish *m/z* 430. This indicates a product in the radiolysis solutions having a molecular weight of 200 g/mol. The fact that no ion corresponding to protonated or natiated versions of this is observed (no *m/z* 201 or 223) indicates that it is not as nucleophilic as CMPO, which out-competes it for the available charge. A key observation is that the adduct at *m/z* 630 increases in relative abundance with increasing absorbed radiation dose (0 to 20 to 38.3 kGy). A hypothesis is that the product is

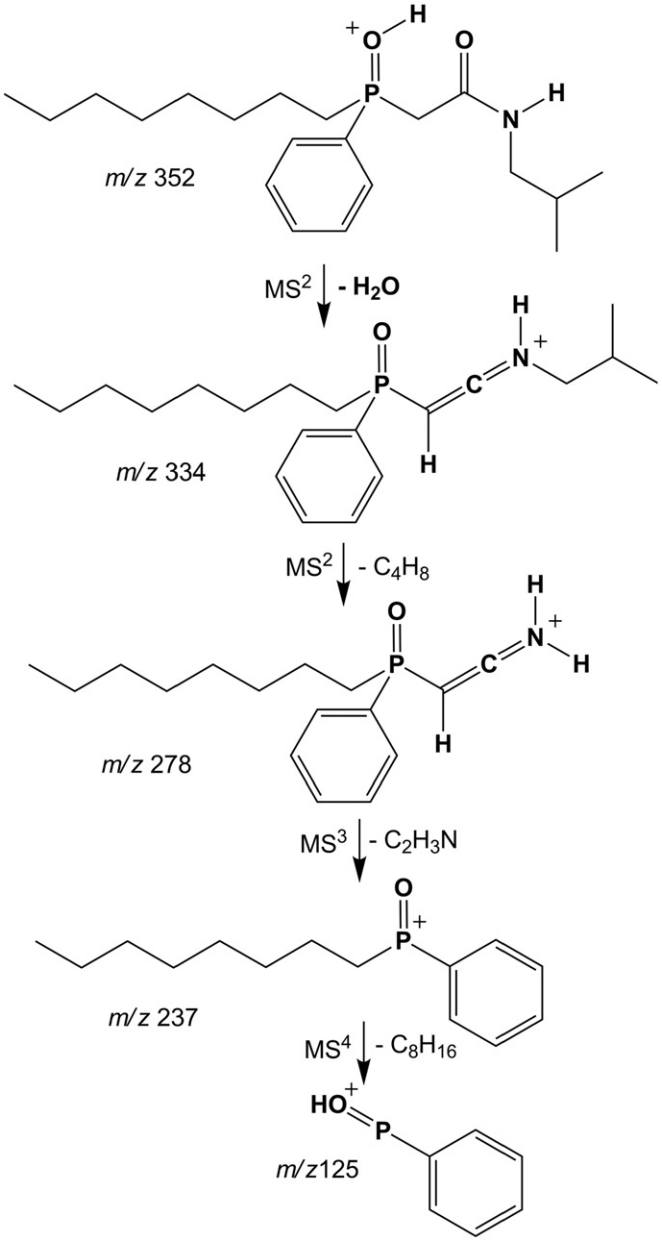

Fig. 9. Proposed fragmentation of the protonated, mono-isobutyl CMPO derivative formed from radiolysis. Note that both *m/z* 334 and 278 are formed in the MS^2 analysis, and are probably serial reactions in the order shown.

O-isopropylphenylphosphonic acid (Fig. 1, cleavages 'a' and 'b', then recombination with *i*-$C_3H_7^{\bullet}$ and $OH^{\bullet}$); however additional support for this idea is required.

Several ions indicate the formation of small amides: N,N-diisobutylformamide (DiBFA) and N,N-diisobutylacetamide (DiBAA) can be formed by cleavages 'c' and 'b', respectively (Fig. 1), followed by recombination with $H^{\bullet}$. Other products corresponding to higher

molecular weight products of these cleavage reactions have been observed previously [18] (and in this study), which is consistent with formation of the amides seen here. A low-abundant ion at *m/z* 565 likely corresponds to an adduct consisting of DiBFA and protonated CMPO, $[(CMPO)(DiBFA)H]^+$. When ion trapping is limited to *m/z* values <400, a low abundance *m/z* 336 is seen, consistent with $[(DiBFA)_2Na]^+$ (Fig. S25).

Further analysis limiting ion trapping to $<m/z$ 200 produced what is likely $[(DiBFA)H]^+$ at *m/z* 158, and $[(DiBAA)H]^+$ at *m/z* 172 (Fig. S25). The ion at *m/z* 186 is the most abundant of this group, and may be formed from recombination of the radical formed from cleavage 'b' (Fig. 1) with a methyl radical.

Direct infusion ESI analysis of NaOH extracts of the alpha-irradiated CMPO–dodecane samples did not provide significant information regarding possible degradation products. On the other hand, analyses of the HNO_3 extracts produced spectra containing abundant HMA, which was added as a surrogate amine. An abundant ion series having the general formula $[(HMA+H)_{n+1}(NO_3)_n]^+$ where $n=0$–3 accounted for *m/z* 116, 294, 472 and 650, respectively (HMA–nitrate clusters, denoted 'hnc' in Fig. 11), while *m/z* 408 and 523 corresponded to protonated CMPO and $[(CMPO)(HMA)H]^+$. Ions at *m/z* 363, 448, 533, and 618 were the $[(NaNO_3)_nNa]^+$ series (sodium nitrate clusters, denoted 'snc').

Two low abundance ions at *m/z* 130 and 308 are indicative of diisobutylamine (DiBA), which is a radiolysis product formed from cleavage of the amide bond (Fig. 1, cleavage 'd'). $[(DiBA)H]^+$ accounts for *m/z* 130, while the complex $[(DiBA)(HMA)NO_3]^+$ accounts for *m/z* 308, which produced fragment ions at *m/z* 130 and 116 (Fig. 11) when dissociated.

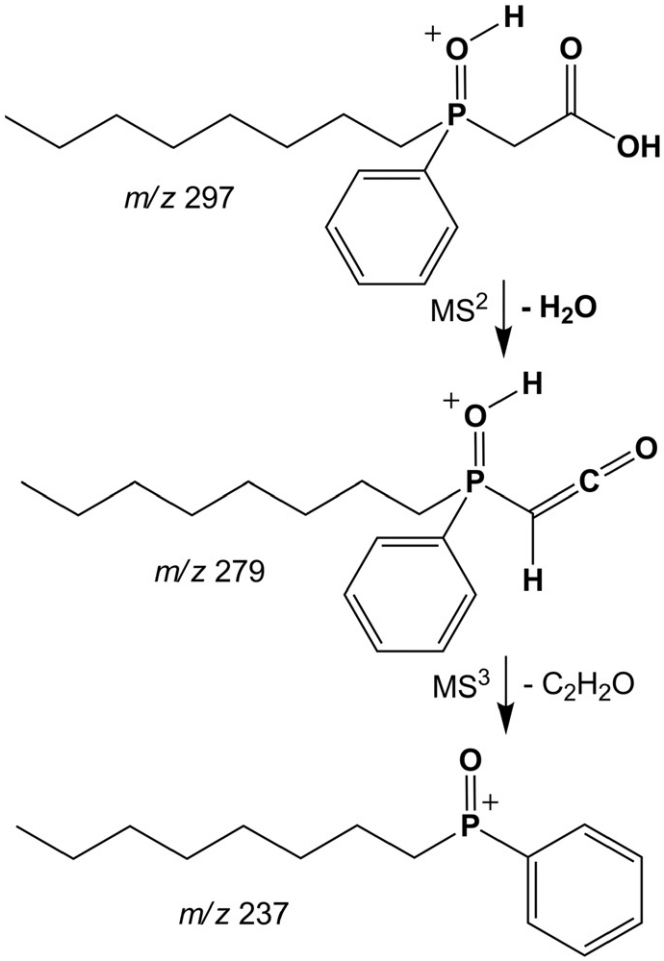

Fig. 10. Proposed structure, and fragmentation scheme for CMPO radiolysis product at *m/z* 297.

4. Discussion

4.1. Degradation product screening using direct infusion ESI-MS

The positive ion spectra are dominated by natiated CMPO ions that make observation of low abundance degradation products difficult, particularly when using a mass analyzer having limited dynamic range. However low abundance degradation products can be observed by restricting ion accumulation so that the quadrupole ion trap is not filled with cationized CMPO species. This approach enabled observation of ions consistent with rational degradation products expected from CMPO radiolysis, and in many cases assignments were supported by the multiple-stage mass spectrometry (MS^n) capability of the quadrupole ion trap. Cluster and complex ions having *m/z* values greater than that of cationized CMPO provided significant information on degradation products that were not observed as simple cationized species; a significant example is the bis-CMPO-HNO_3 complex formed from acid contact and

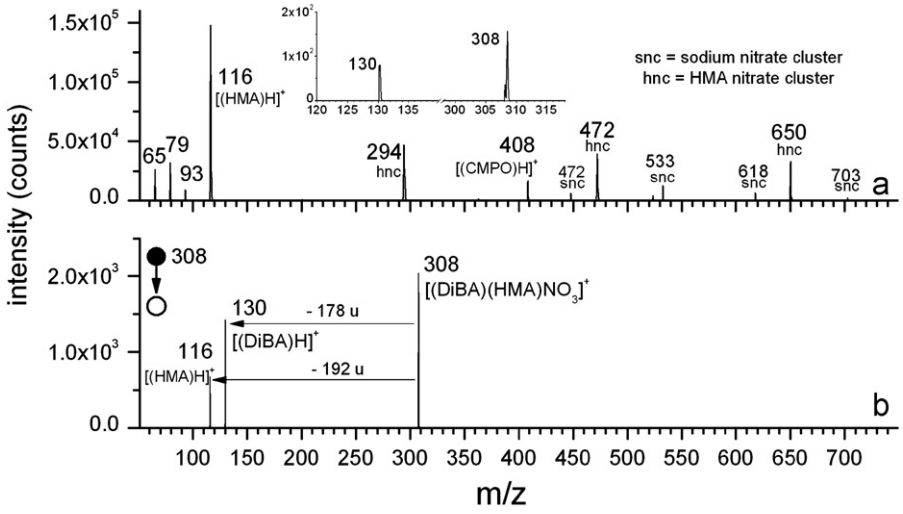

Fig. 11. Positive ESI-MS analysis of the HNO_3 extract of an alpha-irradiated CMPO sample (20 kGy) spiked with HMA. (a) MS^1 spectrum, inset is partial spectrum, expanded *y* axis, split *x* axis. (b) MS^2 of the complex at *m/z* 308.

partitioned into the nitric acid phase. The observation of acidic or basic degradation products was significantly facilitated by using simple NaOH or HNO_3 extractions, respectively. The aqueous extracts were analyzed directly after dilution with methanol, and acidic carboxylate and phosphoryl-containing compounds, and amines were readily observed in the respective extracts.

4.2. Radiolytic dissociation pathways

At present, the direct infusion screening methods do not provide quantitative measurements of the radiolysis products, and so rigorous comparisons of gamma-, versus alpha-induced degradation are beyond the scope of this paper. However, significant differences in the types of products observed suggest that the two radiation-induced degradation processes are not identical. Differences in the degradation pathways experienced by CMPO when irradiated with gamma and alpha sources may be attributed to the differences in linear energy transfer (LET) by the two radiation sources. The low LET gamma radiation favors production of free radical reactive species in the tracks left by the incident photon. These then diffuse into bulk solution to react with ligands such as CMPO. In contrast, the very high LET alpha source produces a high local concentration of radicals which react with each other to form molecular species before they diffuse into solution. As one example, the yield of $^{\bullet}OH$ radical is higher for the low LET radiation, while for the high LET radiation $^{\bullet}OH$ radical addition reactions decrease the yield and increase the yield of H_2O_2 [28]. The effect of these changed yields may be apparent in the degradation products found for the two radiation sources.

The mass spectra of the gamma-irradiated samples contain numerous ions that require cleavage of the amide bond (Fig. 1'd'), including all of the small amine signatures, the acetic acid derivative, and one of the higher mass conjugates. There are also significant indications for cleavage of the phosphoryl–methylene bond, cleavage 'b', notably in the diisobutylacetamide-containing species, and octylphenylphosphinic acid. The rupture of these bonds may be favored by free radical reactions, probably initiated by $^{\bullet}H$ atom abstraction reactions. There is also evidence for cleavage of the octyl ('a'), phenyl, and isobutyl ('e') moieties, but these are less prevalent. The free radicals generated by these homolytic cleavage reactions undergo recombination reactions with other radicals, most often $H^{\bullet}$, $CH_3^{\bullet}$, $C_3H_7^{\bullet}$, and $OH^{\bullet}$. These could be generated from CMPO; however the first three could also be produced from the dodecane solvent used in the irradiation experiments.

Direct infusion ESI mass spectra of the α-irradiated samples contained several ions that were interpreted in terms of diisobutylacetamide and diisobutylformamide, which must be formed from cleavages 'b' and 'c', perhaps initiated by oxidative reaction with H_2O_2. Diisobutylamine was also observed, indicating that cleavage 'd' is also occurring, but the overall amine signature was not as intense as in the mass spectra of the γ-irradiated samples, perhaps reflecting the lower yield of free radical species.

Acknowledgment

This research was funded by the U.S. DOE Office of Nuclear Energy, Fuel Cycle Research and Development program, under DOE Idaho Operations Office contract DE-AC07-99ID13727. Irradiation experiments were performed at the Idaho National Laboratory, and the Radiation Research Laboratory at the University of Notre Dame. Partial funding for this work was also provided by Nuclear Energy Universities Program, under DOE-NEUP program DE-AC07-05ID14517.

Appendix A. Supplementary material

Supplementary data associated with this article can be found in the online version at http://dx.doi.org/10.1016/j.talanta.2012.07.056.

References

[1] S.A. Ansari, P. Pathak, P.K. Mohapatra, V.K. Manchanda, Sep. Purif. Rev. 40 (2011) 43–76.
[2] E.P. Horwitz, D.G. Kalina, H. Diamond, G.F. Vandegrift, W.W. Schulz, Solvent Extr. Ion Exch. 3 (1985) 75–109.
[3] J.N. Mathur, M.S. Murali, K.L. Nash, Solvent Extr. Ion Exch. 19 (2001) 357–390.
[4] M.S. Murali, J.N. Mathur, Solvent Extr. Ion Exch. 19 (2001) 61–77.
[5] W.W. Schulz, E.P. Horwitz, Sep. Sci. Technol. 23 (1988) 1191–1210.
[6] K. Arai, M. Yamashita, M. Hatta, H. Tomiyasu, Y. Ikeda, J. Nucl. Sci. Technol. 34 (1997) 521–526.
[7] R.R. Chitnis, P.K. Wattal, A. Ramanujam, P.S. Dhami, V. Gopalakrishnan, A.K. Bauri, A. Banerji, J. Radioanal. Nucl. Chem. 240 (1999) 721–726.
[8] E.P. Horwitz, H. Diamond, K.A. Martin, R. Chiarizia, Solvent Extr. Ion Exch. 5 (1987) 419–446.
[9] B.J. Mincher, G. Modolo, S.P. Mezyk, Solvent Extr. Ion Exch. 27 (2009) 579–606.
[10] B.A. Buchholz, L. Nunez, G.F. Vandegrift, Sep. Sci. Technol. 31 (1996) 2231–2243.
[11] R. Chiarizia, E.P. Horwitz, Solvent Extr. Ion Exch. 8 (1990) 907–941.
[12] K.L. Nash, R.C. Gatrone, G.A. Clark, P.G. Rickert, E.P. Horwitz, Sep. Sci. Technol. 23 (1988) 1355–1372.
[13] R. Chiarizia, E.P. Horwitz, Solvent Extr. Ion Exch. 4 (1986) 677–723.
[14] K.L. Nash, P.G. Rickert, E.P. Horwitz, Solvent Extr. Ion Exch. 7 (1989) 655–675.
[15] K.L. Nash, R.C. Gatrone, G.A. Clark, P.G. Rickert, E.P. Horwitz, Sep. Sci. Technol. 23 (1988) 1355–1372.
[16] R.C. Gatrone, P.G. Rickert, E.P. Horwitz, B.F. Smith, C.S. Bartholdi, A.M. Martinez, J. Chromatogr. 516 (1990) 395–404.
[17] J.N. Mathur, M.S. Murali, P.B. Ruikar, M.S. Nagar, A.T. Sipahimalani, A.K. Bauri, A. Banerji, Sep. Sci. Technol. 33 (1998) 2179–2196.
[18] G. Elias, G.S. Groenewold, B.J. Mincher, S.P. Mezyk, J. Chromatogr. A 1243 (2012) 47–52.
[19] G.S. Groenewold, D.R. Peterman, J.R. Klaehn, Rapid Commun. Mass Spectrom. 26 (2012) 2195–2203.
[20] G.S. Groenewold, M.J. van Stipdonk, G.L. Gresham, W. Chien, K. Bulleigh, A. Howard, J. Mass Spectrom. 39 (2004) 752–761.
[21] E. Leclerc, D. Guillaumont, P. Guilbaud, L. Berthon, Radiochim. Acta 96 (2008) 85–92.
[22] T.J. Stockmann, Y. Lu, J. Zhang, H.H. Girault, Z.F. Ding, Chem. Eur. J. 17 (2011) 13206–13216.
[23] H. Herschbach, F. Brisach, J. Haddaoui, M. Saadioui, E. Leize, A. Van Dorsselaer, F. Arnaud-Neu, V. Bhomer, Talanta 74 (2007) 39–46.
[24] C. Lamouroux, S. Rateau, C. Moulin, Rapid Commun. Mass Spectrom. 20 (2006) 2041–2052.
[25] G.S. Groenewold, A.D. Appelhans, M.E. McIlwain, G.L. Gresham, Int. J. Mass Spectrom. 301 (2011) 136–142.
[26] G.S. Groenewold, J.J. Gaumet, J. Mass Spectrom. 46 (2011) 1273–1280.
[27] J.C. Ingram, G.S. Groenewold, A.D. Appelhans, J.E. Delmore, D.A. Dahl, Anal. Chem. 67 (1995) 187–195.
[28] B.J. Mincher, G. Modolo, S.P. Mezyk, Solvent Extr. Ion Exch. 27 (2009) 1–25.